ISSN 2303-4521
Periodicals of Engineering and Natural Sciences
Methodology/Method
Vol. 9, No. 4, November 2021, pp.913-920

Design of rotary inverted pendulum swinging-up and stabilizing

Zuhair Shakor Mahmood [1], Imad Burhan Kadhim [2], Ali Najdet Nasret [3]
[1, 2, 3] Electronic Department, Kirkuk Technical Institute, Northern Technical University

ABSTRACT

The mechanical design of inverted pendulum systems may be very diverse. This study makes use of mathematics to explain the expanded unstable Rotary planer inverted pendulum arrangement (Rotary -inverted system). Pin connections are used in planer-inverted pendulums to attach the pendulum to the rotating- Rotary actuation base. This design of a Rotary -inverted pendulum is explored in the development of underactuated robotic systems because it best simulates the balance of a broomstick in the hand by treating the elbow and shoulder as revolute joints. It is necessary to utilize the Lagrangian equation of motion when creating the dynamical equation for the Rotary -inverted pendulum. MATLAB Simulink is used to simulate a nonlinear computational model of the system so as to test the accuracy of the mathematical model.

Keywords: Rotary-Inverted pendulum, Lagrangian, Broomstick.

Corresponding Author:

Zuhair Shakor Mahmood
Electronic Department Kirkuk Technical Institute
Northern Technical University
Kirkuk, Iraq
E-mail: zuherkazanci@ntu.edu.iq

1. Introduction

Because of the intricacy of its modeling, stabilization, and trajectory tracking, this nonlinear and unstable inverted pendulum poses a difficult challenge in contemporary control theory. The mechanics of balancing a pendulum while operating rocket thrusters, aviation systems, marine systems, or space vehicles may be useful for human transporter Segway's and humanoid robots alike. For mechanical engineers, the actuation technique and degree of freedom are critical when constructing an inverted pendulum (DOF). The actuation methods include rotational and linear. Both the base location and the pendulum angle may be varied with inverted pendulum systems, thus they have two degrees of freedom (DOF), systems include the cart inverted pendulum and Rotary inverted pendulum [1-2]. A pin joint is used in an inverted pendulum system to connect a swinging pendulum to a spinning cart, which is subsequently driven by the cart's motor to revolve in the horizontal plane [3–4]. To put it simply, the RIP system is composed of three basic parts: an arm, a pendulum and motor. In Rotary inverted pendulum, a pin joint that allows the pendulum to move about freely in the vertical plane is used to connect the motor shaft to one arm and the pendulum to the other arm, with the motor shaft being attached to one arm and the pendulum being connected to the other arm [5-6]. Mechanism using an inverted pendulum Design options that provide more flexibility enable the base to move in several dimensions or add more pendulum attachments to the design. When the base may move in two directions, there must be two degrees of freedom.. With this system, a horizontal plane has been obtained. It's called "(PIPS)." An inverted pendulum planer may make use of three different mechanical structures: linear-linear actuation, rotational-rotational action, or any combination of the two. Although RIP and cart inverted pendulum systems may be modeled and built, only a few articles have been published on the subject of planning inverted pendulum systems. Cart inverted pendulum system represented by the Lagrangian equation of motion in [7]. Newtonian principles were used to model an inverted cart pendulum system. This spinning inverted pendulum is known as the Furuta pendulum, and its dynamics have been figured out in [8]. A Newton-Euler formulation and Lagrangian equation of motion were used to characterize RIP's nonlinear dynamics. The Furuta pendulum was described in detail by [9-10]. The SolidWorks software and Lagarangian equation of motion were utilized in the construction of the Furuta pendulum mechanical design. Modeling a dual-axis inverted pendulum system with actuator dynamics based on energy conservation was done by [11-16]. For the first time, a robot with just two degrees of freedom has been created by researchers [12]. Was the publication in which they detailed their results. Decoupled or weakly coupled connections were used to attach the pendulum to a SCARA robot. [13-14] used linear and nonlinear control methods to keep an inverted pendulum in a vertically ascending position. [15-17] Describes how to remove the Furuta pendulum's limit cycle. An examination of the literature found that only a small number of writers have attempted to simulate the planer-inverted pendulum. As an alternative to prior techniques that employed decoupled links to bind the pendulum to its rotary-planer actuation base, this work proposes nonlinear computational modeling of a Rotary planer inverted pendulum system using a pin joint (Rotary inverted pendulum system). This setup of a planer with an inverted pendulum is called an inverted pendulum configuration is considered in the research of underactuated robotic systems because it best simulates the balance of a broomstick in the hand by viewing the elbow and shoulder as revolute joints. The Lagrangian mathematical expression is employed in the construction of the model. Numerical simulation of the system's nonlinear model in MATLAB Simulink have been checked the validates of mathematical model [18-19].

2. Structure of the rotary inverted pendulum system

This figure 1 depicts an inverted pendulum that was constructed using a Rotary planer. Arm 1, Arm 2, 3 Pendulum make up the basic structural components. D.C. motor's shaft is connected to arm one, which may move horizontally. In order to produce torque for rotation in the horizontal plane, the revolute joint connecting the first and second arms may be driven by a servo motor. A pin joint connects arm 2 to the pendulum, which may swing freely in the vertical plane. There are three angles shown in Figure 2, one for each arm. The angle q_1 depicts the angle between the first and second arms as measured from an arbitrarily chosen point. The angle q_2 depicts that between second and first arms. The pendulum position is represented by q_3. There are no negative angular displacements in a clockwise direction. m_1, m_2, and m_3 are the mass numbers associated with the first two arms and the pendulum. The two arms are the longest part, followed by the pendulum with an L_2 and an L_3 measurement. The lengths of the first and second arms, as well as the pendulum, are I_1, I_2, and I_3 respectively, measured from the points where the arms and pendulum rotate.

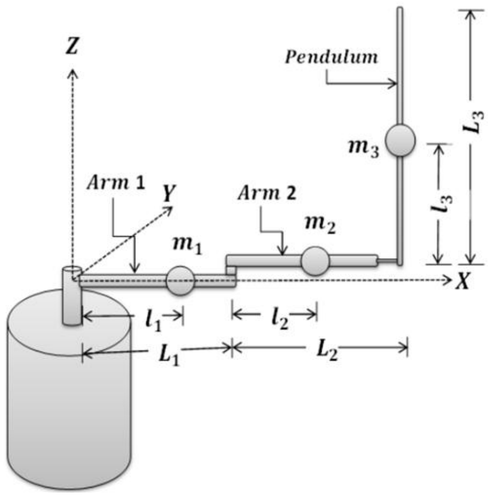

Figure 1. Inverted Pendulum Rotary.

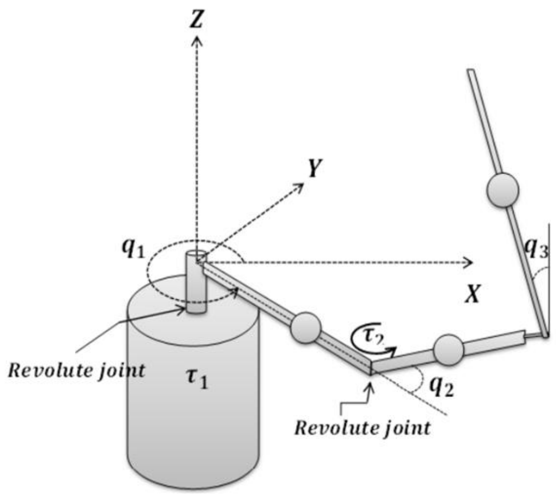

Figure 2. Torque applications and relative joint angle movements are used in the Rotary -inverted pendulum

Using electric motors, torque one and torque two may be applied to arms 1 and 2. When arm 2 is not activated, the pendulum is free to swing in whatever direction it chooses. The inertia tensors of the first and second arms are l1, l2, and l3, respectively (around the mass center). The joint's viscous damping coefficients are b1, b2, and b3.

3. Rotary inverted pendulums Lagrangian formulation

Because it is a three (DOF) system, the inverted Rotary pendulum is subject to three different sets of Lagrangian equations of motion.

$$\frac{d}{dt}\left(\frac{\partial \mathrm{L}}{a\dot{q}_1}\right)-\frac{\partial \mathrm{L}}{aq_1}=\tau_1-b_1\dot{q}_1 \tag{1}$$

$$\frac{d}{dt}\left(\frac{\partial \mathrm{L}}{a\dot{q}_2}\right)-\frac{\partial \mathrm{L}}{aq_2}=\tau_2-b_2\dot{q}_2 \tag{2}$$

$$\frac{d}{dt}\left(\frac{\partial \mathrm{L}}{a\dot{q}_3}\right)-\frac{\partial \mathrm{L}}{aq_3}=-b_3\dot{q}_3 \tag{3}$$

This is the difference between kinetic and potential energy, and where $\mathcal{L}$ is the Lagrangian of system

$$\mathrm{L}=E_k-E_p \tag{4}$$

Kinetic energy in an inverted pendulum system equals E_{k3}, whereas potential energy equals E_p. Potential energy equals the sum of all three energies: kinetic E_k and potential E_p. The kinetic energy is equal to all three energies combined: two arms, a pendulum, and their combined potential energy E_p is equal to all three energies combined. It is assumed that since Arms 1 and 2 move on a horizontal plane, their potential energies are zero.

$$E_{p1}=E_{p2}=0 \tag{5}$$

As illustrated in Figure 3, the pendulum's potential energy allows us to compute

$$E_{p3}=m_3gl_3\left(\cos\left(q_3\right)-1\right) \tag{6}$$

Assuming that arm 1 and arm 2 have equal potential energy, then arm 1's total potential energy is equal to

$$E_p=E_{p1}+E_{p2}+E_{p3} \tag{7}$$

Arm 1's kinetic energy is

$$E_{k1}=\frac{1}{2}m_1v_1^Tv_1+\frac{1}{2}J_1\dot{q}_1^2 \tag{8}$$

As a result, the study's kinematics will need to be examined in order to be comprehensive. This may be seen in Figure 3 where the center of mass of Arm 1 depends on.

$$O_1=\left[x_1,y_1,z_1\right]^T \tag{9}$$

Figure 3(a) shows a free body diagram that defines, and as follows:

$$x_1=l_1\cos\left(q_1\right),y_1=l_1\sin\left(q_1\right),z_1=0$$

In other words, we may say that

$$v_1=\left[\dot{x}_1,\dot{y}_1,\dot{z}_1\right]^T \tag{10}$$

Being

$$\dot{x}_1=-\dot{q}_1l_1\sin\left(q_1\right),\dot{y}_1=\dot{q}_1l_1\cos\left(q_1\right),\dot{z}_1=0$$

Here is what happens when equation (10) is used in place of equation (8), and then the expression is rearranged.

$$E_{k1}=\frac{1}{2}m_1l_1^2\dot{q}_1^2+\frac{1}{2}J_1\dot{q}_1^2 \tag{11}$$

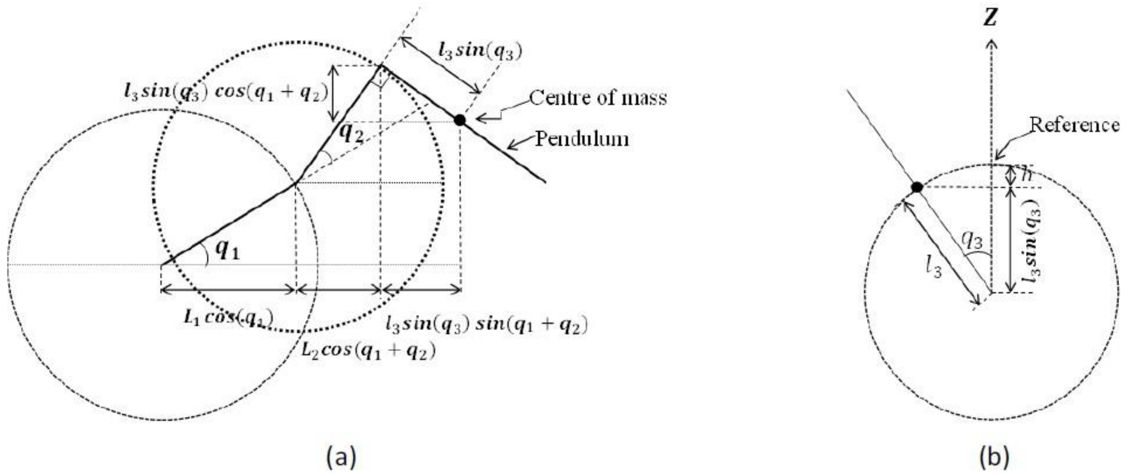

Figure 3. An inverted pendulum's free body Rotary diagram (a) horizontal projection assumption (b) vertical projectile assumption

To calculate the kinetic energy of the second arm and the pendulum, use and, which are indicated in the same manner that was. These are the words that were used to describe them:

$$E_{k2} = \frac{1}{2} m_2 \left[L_1^2 \dot{q}_1^2 + l_2^2 \left(\dot{q}_1 + \dot{q}_2 \right)^2 + 2 L_1 l_2 \dot{q}_1 \left(\dot{q}_1 + \dot{q}_2 \right) \cos\left(\dot{q}_2 \right) \right] + \frac{1}{2} J_2 \left(\dot{q}_1 + \dot{q}_2 \right)^2 \tag{12}$$

$$E_{k3} = \frac{1}{2} J_3 \dot{q}_3^2 + \frac{1}{2} m_3 \begin{bmatrix} L_1^2 \dot{q}_1^2 + l_3^2 \dot{q}_3^2 + \left(\dot{q}_1 + \dot{q}_2 \right)^2 l_3^2 \sin^2\left(q_3 \right) + \left(\dot{q}_1 + \dot{q}_2 \right)^2 L_2^2 \\ -2 \dot{q}_3 \left(\dot{q}_1 + \dot{q}_2 \right) l_3 L_2 \cos\left(q_2 \right) - 2 \dot{q}_1 \dot{q}_3 \cos\left(q_3 \right) \\ +2 \dot{q}_1 \left(\dot{q}_1 + \dot{q}_2 \right) l_3 L_1 \sin\left(q_2 \right) \sin\left(q_3 \right) + 2 \dot{q}_1 \left(\dot{q}_1 + \dot{q}_2 \right) L_1 L_2 \cos\left(q_2 \right) \end{bmatrix} \tag{13}$$

Adding the kinetic energies of the first and second arms, as well as the pendulum, yields the system's total kinetic energy.

$$E_k = E_{k1} + E_{k2} + E_{k3} \tag{14}$$

Equation (4) may be written as follows by substituting the preceding terms kinetic and potential energy values and lowering the resultant expression:

$$\begin{aligned} \mathrm{L} = {} & \frac{1}{2} \dot{q}_1^2 \left[J_1 + m_1 l_1^2 \right] + \frac{1}{2} J_2 \left(\dot{q}_1 + \dot{q}_2 \right)^2 + \frac{1}{2} m_2 \begin{bmatrix} L_1^2 \dot{q}_1^2 + l_2^2 \left(\dot{q}_1 + \dot{q}_2 \right)^2 \\ +2 L_1 l_2 \dot{q}_1 \left(\dot{q}_1 + \dot{q}_2 \right) \cos\left(\dot{q}_2 \right) \end{bmatrix} \\ & + \frac{1}{2} J_3 \dot{q}_3^2 + \frac{1}{2} m_3 \begin{bmatrix} L_1^2 \dot{q}_1^2 + l_3 \dot{q}_3^2 1 + \left(\dot{q}_1 + \dot{q}_2 \right)^2 l_3^2 \sin\left(q_3 \right) + \left(\dot{q}_1 + \dot{q}_2 \right)^2 L_2^2 \\ -2 \dot{q}_3 \left(\dot{q}_1 + \dot{q}_2 \right) l_3 L_2 \cos\left(q_3 \right) - 2 \dot{q}_1 \dot{q}_3 \cos\left(q_2 \right) \cos\left(q_3 \right) \\ +2 \dot{q}_1 \left(\dot{q}_1 + \dot{q}_2 \right) l_3 L_1 \sin\left(q_2 \right) \sin\left(q_3 \right) \\ +2 \dot{q}_1 \left(\dot{q}_1 + \dot{q}_2 \right) L_1 L_2 \cos\left(q_2 \right) \end{bmatrix} - m_3 g l_3 \left(\cos\left(q_3 \right) - 1 \right) \end{aligned} \tag{15}$$

Euler-Lagrange terms are evaluated and substituted in equations 1 through 3 to get these sets of simultaneous differential equations:

$$\begin{bmatrix} \left(M_{11} \ddot{q}_1 + M_{12} \ddot{q}_2 + M_{13} \ddot{q}_3 + C_{11} \dot{q}_1 + C_{12} \dot{q}_2 + C_{13} \dot{q}_3 + G_1 + F_{v1} \right) \\ \left(M_{21} \ddot{q}_1 + M_{22} \ddot{q}_2 + M_{23} \ddot{q}_3 + C_{21} \dot{q}_1 + C_{22} \dot{q}_2 + C_{23} \dot{q}_3 + G_2 + F_{v2} \right) \\ \left(M_{31} \ddot{q}_1 + M_{32} \ddot{q}_2 + M_{33} \ddot{q}_3 + C_{31} \dot{q}_1 + C_{32} \dot{q}_2 + C_{33} \dot{q}_3 + G_3 + F_{v3} \right) \end{bmatrix} = \begin{bmatrix} \tau_1 \\ \tau_2 \\ 0 \end{bmatrix} \tag{16}$$

Where

$$M_{11}=J_1+J_2+m_1l_1^2+m_2L_1^2+m_2l_2^2+m_3L_1^2+m_3L_2^2+2m_2L_1L_2\cos(q_2)+m_3l_3^2\sin^2(q_3)$$
$$+2m_3l_3L_1\sin(q_2)\sin(q_3)+2m_3L_1L_2\cos(q_2),$$
$$M_{12}=J_2+m_2l_2^2+m_3L_2^2+m_2L_1l_2\cos(q_2)+m_3l_3L_1\sin(q_2)\sin(q_3)+m_3L_1L_2\cos(q_2)$$
$$+m_3l_3^2\sin^2(q_3),$$
$$M_{13}=-m_3L_2l_3\cos(q_3)-m_3l_3L_1\cos(q_2)\cos(q_3),M_{21}=M_{12},$$
$$M_{22}=J_2+m_2l_2^2+m_3L_2^2+m_3l_3^2\sin^2(q_3),$$
$$M_{23}=-m_3L_2l_3\cos(q_3),$$
$$M_{31}=M_{13},M_{32}=M_{23},M_{33}=J_3+m_3l_3^2,$$
$$C_{11}=-2\dot{q}_2m_2L_1l_2\sin(q_2)+\dot{q}_3m_3l_3^2\sin(2q_2)+2\dot{q}_2m_3l_3L_1\cos(q_2)\sin(q_3)$$
$$+2\dot{q}_3m_3l_3L_1\sin(q_2)\cos(q_3)-2\dot{q}_2m_3L_1L_2\sin(q_2),$$
$$C_{12}=-\dot{q}_2m_2L_1l_2\sin(q_2)+\dot{q}_3m_3l_3^2\sin(2q_3)-2\dot{q}_3m_3l_3L_1\sin(q_2)\cos(q_3)$$
$$+\dot{q}_2m_3l_3L_1\cos(q_2)\sin(q_3)-\dot{q}_2m_3L_1L_2\sin(q_2),$$
$$C_{13}=\dot{q}_3m_3L_2l_3\sin(q_3)+\dot{q}_3m_3l_3L_1\sin(q_3)\cos(q_2),$$
$$C_{21}=-3\dot{q}_2m_2L_1l_2\sin(q_2)+\dot{q}_3m_3l_3^2\sin(2q_3)-2\dot{q}_1m_2L_1l_2\sin(q_2)$$
$$-\dot{q}_1m_3l_3L_1\sin(q_3)\cos(q_2)+\dot{q}_1m_3L_1L_2\sin(q_2),$$
$$C_{22}=\dot{q}_3m_3l_3^2\sin(2q_3),C_{23}=\dot{q}_3m_3l_3L_2\sin(q_3),$$
$$C_{31}=\dot{q}_3m_3l_3L_1\cos(q_2)\cos(q_3)+\frac{1}{2}\dot{q}_1m_3l_3^2\sin(2q_3)+\dot{q}_2m_3l_3^2\sin(2q_2)$$
$$-\dot{q}_1m_3l_3L_1\sin(q_3)\cos(q_2)-\dot{q}_1m_3l_3L_1\sin(q_3)\sin(q_2),$$
$$G_1=0,G_2=0,G_3=-m_3gl_3\sin(q_3),F_{v1}=b_1\dot{q}_1,F_{v2}=b_2\dot{q}_2,F_{v3}=b_3\dot{q}_3.$$

4. Hypothesis for an inverted pendulum rotary simulation

The Rotary inverted pendulum system's nonlinear dynamical equation (16) was modelled in MATLAB. Key parameters such as q_1, q_2 and q_3 will be estimated using an inverted pendulum simulation, and the results will be utilized to better understand the system's behavior. Table1 shows the assumed and actual values for the Rotary -inverted pendulum's parameters based on the fundamental (RIP) system features. It is not uncommon for labs to have this experimental set-up available to them.

Table 1. Parameters for the Rotary inverted pendulum system numerical

Symbol	Value	Units
g	9.81	m/s^2
b_1	0.0002	Nms
b_2	0.00017	Nms
b_3	0.00027	Nms
L_1	0.1318	M
L_2	0.09312	M

Symbol	Value	Units
L_3	0.49	M
l_1	$L_1/2$	M
l_2	$L_2/2$	M
l_3	$L_3/2$	M
m_1	0.059	Kg
m_2	0.03946	Kg
m_3	0.041	Kg
J_1	1.076×10^{-4}	$Kg.m^2$
J_2	3.0381×10^{-5}	$Kg.m^2$
J_3	9.9561×10^{-4}	$Kg.m^2$

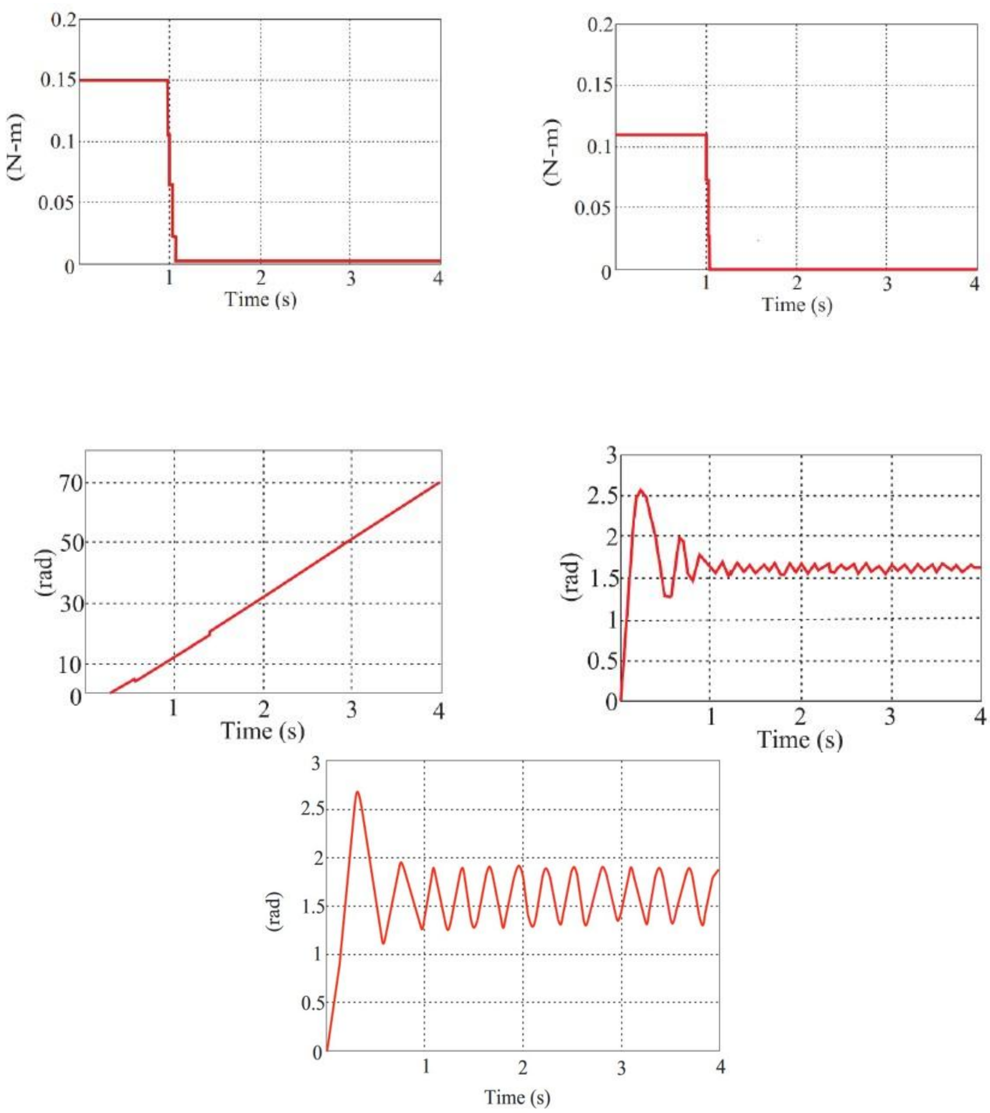

Figure 4. Inverted pendulum system with rotary-rotary-planer response

Using the numerical simulation, the pendulum is shown in Figure 4 beginning at the 0 radian line, which is vertically upward. τ_1 = 0.15 Nm and τ_2 = 0.13 Nm is applied for one second to actuating arm 1 and then for another second to actuating arm 2. The pendulum will swing from its vertically upright position at a radius of around 1.57 percent of its initial length if you put strain on the arms. An in-depth look at the simulation's results can be seen in Figure 4. Draw a picture of the spinning arms 1 and 2 of the system. Torque is given to the first and second arms, and their motion is shown. A radian angle of about 1.57 can be seen in Image 4, since the pendulum has no stabilizing mechanism to prevent it from straying off its unstable vertical equilibrium position

5. Conclusion

A rotary planer system with an inverted pendulum is modeled and simulated in detail in this analysis by beginning with the Lagrangian equation of motion and created computational models. Geometrical projections in the horizontal and vertical planes were supplied to depict the location of the pendulum and arms in computational model. the MATLAB-Simulink have been used to nonlinear model and simulacrated Because the location of the planer inverted pendulum system matches that of the Rotary inverted pendulum system described by the computational model for the Rotary inverted pendulum system provided in this work will succeed.

References

[1] F. Grasser, A. D'arrigo, S. Colombi, and A. C. Rufer, “JOE: a mobile, inverted pendulum,” *IEEE Transactions on industrial electronics,* vol. 49, no. 1, pp. 107-114, 2002.

[2] N. Muskinja and B. Tovornik, "Swinging up and stabilization of a real inverted pendulum," in IEEE Transactions on Industrial Electronics, vol. 53, no. 2, pp. 631-639, April 2006.

[3] K. Pathak, J. Franch and S. K. Agrawal, "Velocity and position control of a wheeled inverted pendulum by partial feedback linearization," in IEEE Transactions on Robotics, vol. 21, no. 3, pp. 505-513, June 2005.

[4] M. Antonio-Cruz, V. M. Hernández-Guzmán and R. Silva-Ortigoza, "Limit Cycle Elimination in Inverted Pendulums: Furuta Pendulum and Pendubot," in IEEE Access, vol. 6, pp. 30317-30332, 2018.

[5] S. Jung and S. S. Kim, "Control Experiment of a Wheel-Driven Mobile Inverted Pendulum Using Neural Network," in IEEE Transactions on Control Systems Technology, vol. 16, no. 2, pp. 297-303, March 2008.

[6] H. Pang and L. Wang, "Robust approximate optimal sliding mode control for a class of affine nonlinear systems with uncertainties," Proceedings of the 29th Chinese Control Conference, 2010, pp. 1657-1662.

[8] N. R. Gans and S. A. Hutchinson, "Visual Servo Velocity and Pose Control of a Wheeled Inverted Pendulum through Partial-Feedback Linearization," 2006 IEEE/RSJ International Conference on Intelligent Robots and Systems, 2006, pp. 3823-3828.

[9] A. Aaref,and Z .Mahmood, "Optimization the Accuracy of FFNN Based Speaker Recognition System Using PSO Algorithm," (2021) International Journal on Communications Antenna and Propagation (IRECAP), 11 (4), pp. 253-260,2021.

[10] A. Nasret and Z. Mahmood, "Optimization and Integration of RFID Navigation System by Using Different Location Algorithms, “International Review of Electrical Engineering (IREE), 14 (4), pp. 291-30,2019.

[11] İ. Uyanık, Ö. Morgül and U. Saranli, "Experimental Validation of a Feed-Forward Predictor for the Spring-Loaded Inverted Pendulum Template," in IEEE Transactions on Robotics, vol. 31, no. 1, pp. 208-216, Feb. 2015.

[12] Y. Tsai, W. Lin, K. B. Cheng, J. Lee and T. Lee, "Real-Time Physics-Based 3D Biped Character Animation Using an Inverted Pendulum Model," in IEEE Transactions on Visualization and Computer Graphics, vol. 16, no. 2, pp. 325-337, March-April 2010..

[13] C. Yang, Z. Li, R. Cui and B. Xu, "Neural Network-Based Motion Control of an Under actuated Wheeled Inverted Pendulum Model," in IEEE Transactions on Neural Networks and Learning Systems, vol. 25, no. 11, pp. 2004-2016, Nov. 2014.

[14] J. Tang and G. Ren, "Modeling and simulation of a flexible inverted pendulum system," in Tsinghua Science and Technology, vol. 14, no. S2, pp. 22-26, Dec. 2009.

[15] E. Q. Ahmed, I. A. Aljazaery, A. F. Al-zubidi, and H. T. S. ALRikabi, “Design and implementation control system for a self-balancing robot based on internet of things by using Arduino microcontroller,” *Periodicals of Engineering Natural Sciences,* vol. 9, no. 3, pp. 409-417, 2021.

[16] T.-D. Chu, and C.-K. Chen, “Design and implementation of model predictive control for a gyroscopic inverted pendulum,” *Applied sciences,* vol. 7, no. 12, pp. 1272, 2017.

[17] Z.S.Mahmood, A.N.Nasret, and O.T. Mahmood, “Separately excited DC motor speed using ANN neural network,” In AIP Conference Proceedings , vol. 2404, no. 1, p. 080012,2021.

[18] Z. S. Mahmood, A. N. N. Coran and A. Y. Aewayd, "The Impact of Relay Node Deployment In Vehicle Ad Hoc Network: Reachability Enhancement Approach," 2019 Global Conference for Advancement in Technology (GCAT),IEEE, ,pp. 1-3, 2019.

[19] Z. S. Mahmood, A. N. N. Coran, A. esam Kamal, and A. B. Noori, "Dynamic Spectrum Sharing is the Best Way to Modify Spectrum Resources." 2021 Asian Conference on Innovation in Technology (ASIANCON), IEEE, pp. 1-5, 2021